Electronic Supplementary Information

Fast kinetics of monoclinic VO_2(B) bulk upon magnesiation via DFT+U calculation

Danmei Gao[a], Jingren Dong[e], Renchao Xiao[a,d], Bo Shang[a], Danmei Yu[a], Changguo Chen[a], Yuping Liu*[a,b,c,e], Kai Zheng*[c], Fusheng Pan[b]

[a.] *College of Chemistry and Chemical Engineering, Chongqing University, Chongqing, 400044, PR China, E-mail:liuyuping@cqu.edu.cn*

[b.] *National Engineering Research Centre for Magnesium Alloys, Chongqing University, Chongqing, 400044, China,*

[c.] *State Key Laboratory of Coal Mine Disaster Dynamics and Control, Chongqing University, Chongqing, 400044, PR China, E-mail:zkcqu@cqu.edu.cn*

[d.] *Huading Guolian Sichuan Automotive Battery Co. Ltd.,Chengdu, 610399, PR China, E-mail::1053576360@qq.com*

[e.] *Chongqing Key Laboratory of Materials Surface & Interface Science, Chongqing University of Arts and Sciences, Chongqing 402160, China, E-mail: dongjingren@cqu.edu.cn*

AUTHOR INFORMATION

Corresponding author:

Name: Yuping Liu

Tel: +86 13594157660

E-mail: liuyuping@cqu.edu.cn

Name: Kai Zheng

E-mail: zkcqu@cqu.edu.cn

1. Supporting Figure

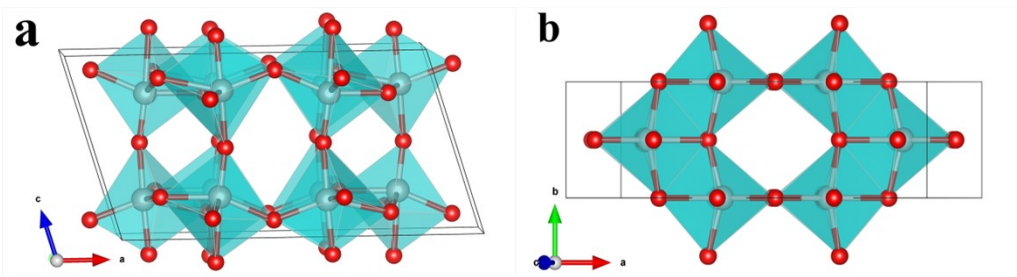

Fig. S1. Polyhedron configurations of VO_2(B) crystal: (a) (010) direction; (b) (001) direction.

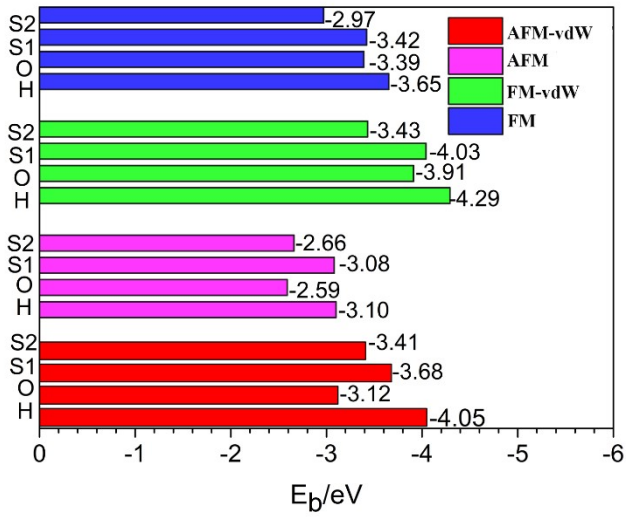

Fig. S2 The binding energies E_b of a single magnesium ion insertion into the 1 × 1 × 2 supercell of VO_2(B) in different calculation conditions.

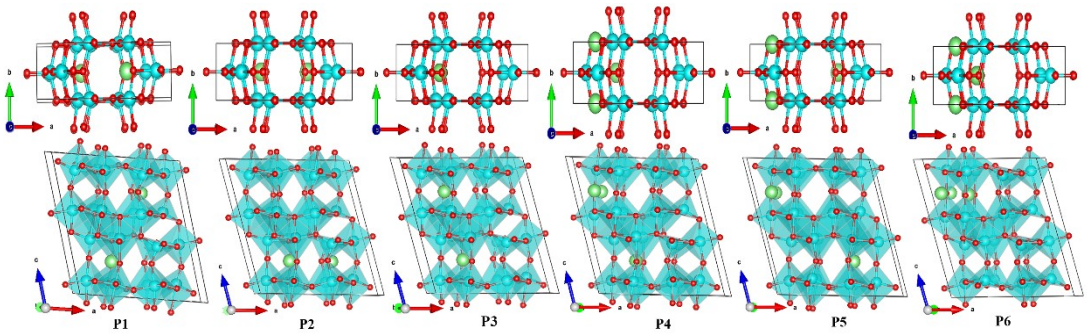

Fig. S3 Various configurations of $Mg_{0.125}VO_2$(B) in the FM and AFM states.

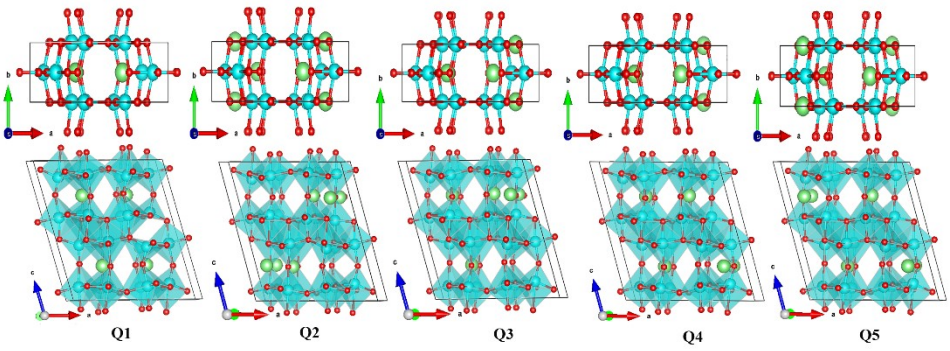

Fig. S4 Different configurations of $Mg_{0.25}VO_2$(B) in the FM states

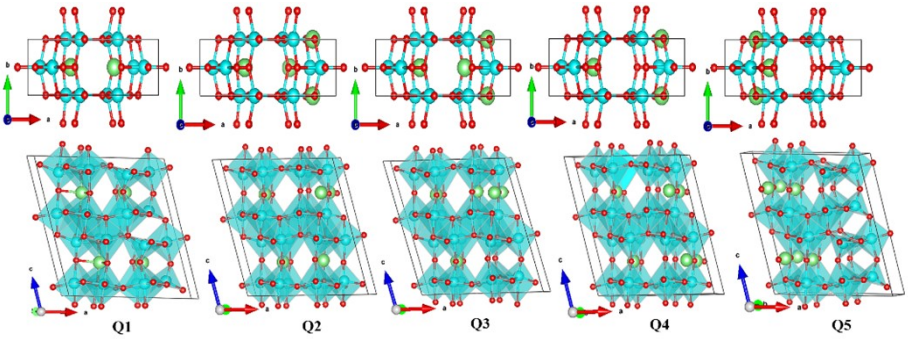

Fig. S5 Different configurations of $Mg_{0.25}VO_2$(B) in the AFM states

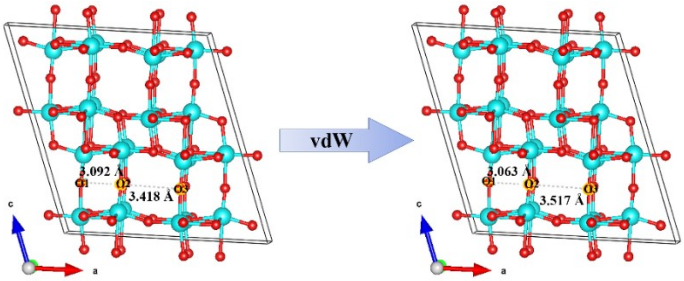

Fig. S6 O-O distance evolution near the diffusion path with and without van der Waals forces

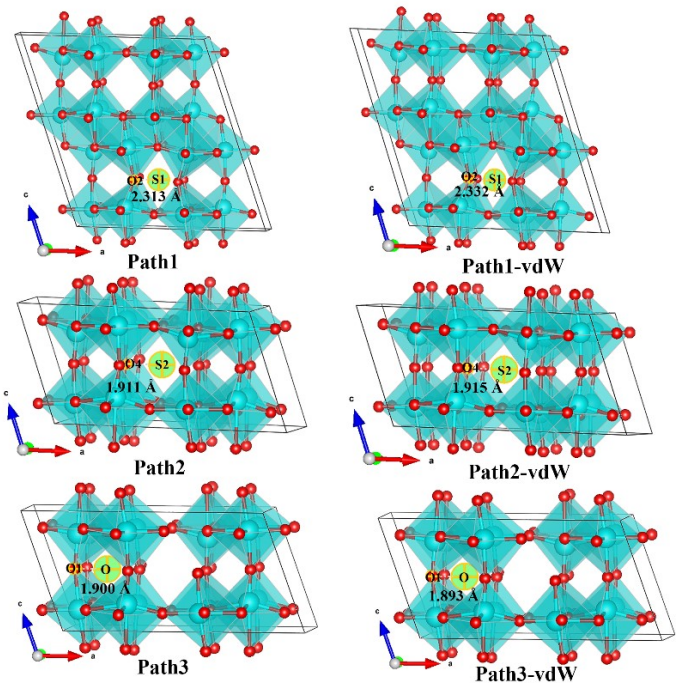

Fig. S7 The transition state configurations with the highest energy barrier in respective pathways and the corresponding distances between Mg^{2+} and surrounding O atom

2. Supporting Tables

Table. S1 Optimized and experimental lattice parameters/energies of 1 × 1 × 2 supercell for VO_2(B) in the four states

	a(Å)	b(Å)	c(Å)	V(Å^3)	Er (%)	Energy(eV)
Exp	12.03	3.693	12.84	546.67	-	-
FM	12.10	3.74	13.31	579.45	6.00	-350.49
FM-vdW	12.09	3.74	13.31	579.44	6.00	-359.66
AFM	12.26	3.86	12.84	582.87	6.62	-351.04
AFM-vdW	12.16	3.83	12.78	572.45	4.71	-360.31

Table. S2 The formation energies of $Mg_{0.125}VO_2$(B) in different configurations

$Mg_{0.125}VO_2$(B)	E_f (P1)/eV	E_f (P2)/eV	E_f (P3)/eV	E_f (P4)/eV	E_f (P5)/eV	E_f (P6)/eV
FM-vdW	-3.37	-3.23	-3.14	-2.95	-3.09	-2.76
AFM-vdW	-1.66	-1.87	-2.05	-1.86	-1.94	-1.35

Table. S3 The formation energies of $Mg_{0.25}VO_2$(B) in different configurations

$Mg_{0.25}VO_2$(B)	E_f (Q1)/eV	E_f (Q2)/eV	E_f (Q3)/eV	E_f (Q4)/eV	E_f (Q5)/eV
FM-vdW	-6.35	-6.11	-6.12	-5.85	-5.77
AFM-vdW	-5.16	-5.09	-5.00	-5.37	-5.02

Table. S4 The formation energies of Mg_xVO_2(B) ($0 \leqslant x \leqslant 1.25$) in the FM-vdW, AFM-vdW, FM and AFM states

Mg_xVO_2(B)	$E_{FM\text{-}vdW}$(eV)	$E_{AFM\text{-}vdW}$(eV)	E_{FM}(eV)	E_{AFM}(eV)
$Mg_{0.125}VO_2$(B)	-371.71	-371.40	-361.04	-361.34
$Mg_{0.25}VO_2$(B)	-383.80	-383.51	-372.54	-371.68
$Mg_{0.5}VO_2$(B)	-406.50	-406.80	-393.60	-393.60
$MgVO_2$(B)	-438.37	-439.34	-421.35	-422.95
$Mg_{1.25}VO_2$(B)	-453.09	-454.84	-432.71	-434.25

Table. S5 The jumping distance starting from the initial state during the Mg^{2+} migration process

Images	1	2	3	4	5	6	7	8
Path1	0.55 Å	1.05 Å	1.54 Å	2.05 Å	2.57 Å	3.05 Å	3.55 Å	4.10 Å
Path1-vdW	0.52 Å	1.00 Å	1.45 Å	1.94 Å	2.44 Å	2.89 Å	3.36 Å	3.88 Å
Path2	0.43 Å	0.92 Å	1.47 Å	2.02 Å	2.51 Å	2.94 Å	3.31 Å	3.68 Å
Path2-vdW	0.37 Å	0.79 Å	1.28 Å	1.84 Å	2.39 Å	2.88 Å	3.30 Å	3.67 Å
Path3	0.54 Å	1.24 Å	1.94 Å	2.47 Å	2.51 Å	2.86 Å	3.33 Å	3.68 Å
Path3-vdW	0.56 Å	1.32 Å	2.12 Å	2.70 Å	2.64 Å	2.97 Å	3.48 Å	3.76 Å